Developmental and Comparative Immunology 177 (2026) 105578

Contents lists available at ScienceDirect

Developmental and Comparative Immunology

journal homepage: www.elsevier.com/locate/devcompimm

Ontogenesis of coelomocyte subsets and immune-related genes during *Eisenia andrei* embryogenesis

Kornélia Bodó [a,1,3], Bohdana Kokhanyuk [a,3], Dániel Dunai [b], Chayeen Brotzki da Costa [a], Éva Rumpler [b,2], Zoltán Kopasz [1], Edit Pollák [b], Péter Németh [a], László Molnár [c], Péter Engelmann [a,*]

[a] Department of Immunology and Biotechnology, Medical School, Clinical Center, University of Pécs, H-7624, Pécs, Hungary
[b] Department of Comparative Anatomy and Developmental Biology, Institute of Biology, Faculty of Sciences, University of Pécs, H-7624, Pécs, Hungary
[c] HUN-REN, Ecophysiological and Ecotoxicological Research Group, Balaton Limnological Research Institute, H-8237, Tihany, Hungary

ARTICLE INFO

Keywords:
Antimicrobial proteins
Coelomocytes
Differentiation
Earthworm
Embryo
Immune response
Pattern recognition molecules

ABSTRACT

Earthworm coelomocytes (e.g. amoebocytes and eleocytes) participate in diverse physiological processes from nutrition storage to immune defense. While the morphology and functional attributes of adult coelomocytes have been extensively studied, their origin and ontogeny are largely unexplored during earthworm development. To uncover this knowledge gap, we examined the emergence, distribution, and molecular characteristics of amoebocytes *vs.* eleocytes during embryogenesis (E1-E4 stages) of *Eisenia andrei* earthworms. Applying light-microscopy and flow cytometry, we observed a sequential manifestation of coelomocyte subsets: amoebocytes predominated in E3 stage, whereas eleocytes became more abundant in E4; although amoebocytes remain prevalent overall. In parallel, the expression dynamics of key earthworm immune-related genes evidenced characteristic differences. The transcripts of evolutionarily conserved *TLR* and *MyD88* displayed constitutive expression throughout all embryonic stages (E1-E4). Conversely, *LBP/BPI* gene expression decreased, while *CCF* mRNA level increased during *Eisenia* embryogenesis. Moreover, antimicrobial effectors (*lysenin* and *lysozyme*) were progressively increased from E1 to E4 stages. Our novel experimental data shed more light at molecular and cellular levels into the development and maturation of immune cell populations during earthworm embryogenesis.

1. Introduction

Adult annelids display a great diversity of body plans, but they share a remarkably conserved developmental pattern, the so-called holoblastic, spiral cleavage. Spiral cleavage of annelids is considered an ancestral feature in bilaterian evolution. In this regard, oligochaete earthworms, as associates of this important phylum, may denote a good model for studying the ontogenesis of major morphogenetic events (e.g. segmentation, mesoderm formation) during bilaterian phylogenesis (Shankland and Seaver, 2000). The process of earthworm embryogenesis has been well documented in several species (Shimizu and Nakamoto, 2001); however, these observations are mostly restricted to the morphological and cytochemical aspects (Bergter et al., 2004). The spiral development of earthworms is accomplished in a specialized morphological structure known as the cocoon. The cocoon is formed by the clitellum (a gland cell-rich segmented area), and it contains the fertilized egg(s) (approx. 100-120 μm in *Eisenia fetida*) along with a large amount of albumin (Bergter et al., 2004). Following earthworm fertilization, the embryonic development can be divided into four major structurally distinct stages (E1-E4, respectively, see Fig. S1) (Boros et al., 2008). Despite the comprehensive description of morphological events, our understanding of the molecular aspects of earthworm ontogenesis remains limited to certain neurotransmitters and some morphogenic factors (Endo et al., 2016; Koza et al., 2006; Matsuo et al., 2005).

Lophotrochozoan annelids are triploblastic organisms composed of three germ layers (ectoderm, endoderm, and mesoderm). One of their

* Corresponding author. Department of Immunology and Biotechnology, Clinical Center, University of Pécs, Pécs, H-7643, Szigeti u. 12, Hungary.
E-mail address: engelmann.peter@pte.hu (P. Engelmann).
[1] National Laboratory of Virology, Szentágothai Research Center, University of Pécs, H-7624 Pécs, Hungary.
[2] Laboratory of Reproductive Neurobiology, HUN-REN Institute of Experimental Medicine, H-1083 Budapest, Hungary.
[3] These authors contributed equally to the performed experiments presented in the manuscript.

https://doi.org/10.1016/j.dci.2026.105578
Received 5 December 2025; Received in revised form 23 January 2026; Accepted 25 February 2026
Available online 26 February 2026

structural novelties is the coelom or secondary body cavity that is formed by hollowing out of a solid cord of mesoderm derived cells or mesothelium. In earthworms, the coelomic cavity is filled with a protein-rich fluid, the coelomic fluid, which plays a central role in several essential physiological processes, including nutrition, osmoregulation, respiration, and immune defense (Vetvicka, 1994). Various cellular components (coelomocytes) are floating in the coelomic cavity to maintain the humoral and cellular immune response (e.g. phagocytosis, encapsulation, ETosis) against the invading pathogens (Homa, 2018). Based on their morphological and functional characterization, coelomocytes have been generally subdivided into two major subtypes (amoebocytes and eleocytes, respectively). Amoebocytes participate in the cellular immune response, while eleocytes play a more prominent role in humoral immunity and nutrient storage (Engelmann et al., 2016). Compared to other protostome mesodermal immune cell populations (e.g. hemocytes), relatively little is known about the origin and ontogeny of coelomocytes during earthworm development (Hartenstein, 2006; Santocki et al., 2014). According to Jamieson (1981), earthworm amoebocyte development is maintained by the peritoneal lining of the coelomic cavity. In each segment, the coelomic cavity is connected to both the parietal layer (somatopleure) and to the visceral layer (splanchnopleure). It has been proposed that amoebocytes emerged from these peritoneal cell layers (Jamieson, 1981), which was supported by subsequent studies (Cooper and Stein, 1981; Dvořák et al., 2016; Engelmann et al., 2005). In contrast, the exact developmental origin of eleocytes is rather debated; however, several pieces of evidence propose that this cell type is derived from the chloragogen tissue of the gut (Opper et al., 2013; Santocki et al., 2014). The chloragogen tissue is composed of sessile cells, which are known as chloragocytes. It seems that circulating eleocytes represent terminally differentiated chloragocytes released into the coelomic cavity (Jamieson, 1981).

Despite detailed descriptions of adult coelomocyte subpopulations, the sequential appearance of the distinct coelomocyte subsets during the development of *E. andrei* remains relatively unknown. To trace the occurrence of amoebocytes *vs*. eleocytes during embryogenesis, we isolated coelomocytes from the different developmental stages (E1-E4, respectively) and analyzed them by various microscopic and light-scatter-based assays. Furthermore, to gain insights into the molecular immune fingerprints of developing embryos, we measured the expression patterns of various immune-related genes (pattern recognition receptors and antimicrobial molecules) across the embryonic stages of *E. andrei* earthworms.

2. Materials and methods

2.1. Earthworms

Mature (clitellated) *Eisenia andrei* (Oligochaeta, Lumbricidae) earthworms were maintained at standard laboratory conditions at room temperature (21 °C) and fed with moist compost and manure soil (Molnár et al., 2012).

2.2. Isolation of embryos and determination of their developmental stages

Cocoons were covered by an earthworm physiological solution (70 mM NaCl, 4 mM KCl, 3 mM $CaCl_2$, 0.35 mM $MgCl_2$, 1.25 mM Tris, 20 mM glucose, pH: 7.3), affixed to a Sylgard plate with minutien pins and had their shell opened with microscissors (Fine Science Tools, Heidelberg, Germany). Thereafter, the albumen was gently shaken off the body surface. Similarly to Boros et al. (2008), the embryonic developmental stages were determined by accurate observation of characteristic morphological landmarks, like body form, development of the central nervous system, metanephridia, and segments, as it can be seen in Fig. S1. Additional key features were the appearance of the main blood vessels - ventral and dorsal ones - further the segmental vessels. To demonstrate the distinct developmental stages, isolated embryos were fixed in a freshly prepared Boer fixative solution (a mixture of 3 mL cc. picric acid, 1 mL of 25% glutaraldehyde and 40 μL of cc. acetic acid) for 3 h at room temperature then washed in 80% ethanol for 1 h and several changes of 0.1 M phosphate buffer for 24 h (Merck Life Sciences, Budapest, Hungary). Microphotos were taken with a Nikon stereomicroscope. The embryos identified with various developmental stages were subsequently used for either coelomocyte extraction or histological processing.

For quantitative gene expression analysis in earthworm embryos, please see the Supplementary Material.

2.3. Extraction and processing of embryonic coelomocytes

The cleaned embryos (8-8 specimens from the E2, E3 and E4 developmental stages) were placed into a drop (25 μL) of the extraction buffer (71.2 mM NaCl, 5 mM EGTA, 50.4 mM guaiacol glyceryl ether, 5% ethanol, pH: 7.3) on a slide for a minute for coelomocyte isolation (Engelmann et al., 2005), then dispersed with a pin to an area of about 1 cm^2. Since E2 specimens did not eject coelomocytes, smear preparations were only taken from E3 and E4 embryos. After 3 min, when coelomocytes had attached to the slide surface, the extraction buffer was quickly absorbed with a filter paper. Isolated embryonic coelomocytes were then further processed according to the downstream analytical applications (please see section 2.4.).

2.4. Enumeration and DIC microscopy of distinct coelomocyte types

Four preparations of each developmental stage were covered with a drop of earthworm physiological saline and coverslipped for differential interference contrast (DIC) microscopy (Nikon Optiphot-2). The rest of smears were covered with a drop of the freshly prepared mixture of formol-acetic acid (FAa) solution (6 mL of 38% formaldehyde, 1 mL of concentrated acetic acid and 18 mL of distilled water) for 10 min, stained with Mayer's haematoxylin and 0.5 % eosin (Merck Life Sciences), then dehydrated and cleared as usual for conventional histology. Twenty-twenty microphotos (200× magnification) were taken from each *in vivo* smear preparation with DIC illumination. More than 400 coelomocytes were counted in the preparations of both E3 and E4 embryos. The number and ratio of distinct coelomocyte types were determined by direct visual observation based on their cytological characteristics.

2.5. Processing of the embryos for histological observation and microscopy

Isolated embryos (5-5 specimens from E2, E3, and E4 developmental stages) were anaesthetised in carbonated water until they were motionless, then were fixed in the freshly prepared FAa solution for 3 days at room temperature. The fixed samples were then washed thoroughly in distilled water and dehydrated in ascending propanol solutions ranging from 70% to 100%, immersed in benzene, and embedded in paraffin as usual. Sections with 10 μm were made by a rotary microtome and treated as usual, then stained with Mayer's haematoxylin and 0.5 % eosin. Sections and smear preparations were investigated with a Nikon Optiphot-2 microscope.

2.6. Flow cytometry

Isolation of E3 and E4 coelomocytes for flow cytometry was performed as we described in section 2.3. Flow cytometry analysis of pooled embryonic coelomocytes was carried out with a FACSCalibur flow cytometer (Beckton Dickinson, Franklin Lakes, NJ, USA). During experiments, 30,000 events per sample were measured based on their forward scatter (FSC) and sideward scatter (SSC) characteristics. Results were analyzed with FCS Express software (De Novo Software, Glendale, CA, USA).

2.7. Statistical analysis

Statistical analyses were carried out with Prism v5.0 (GraphPad Software, La Jolla, CA, USA). Distribution of normality was overseen prior to additional statistical tests (Shapiro-Wilk Normality Test). In the case of normal distribution, one-way ANOVA followed by Bonferroni multiple comparison post hoc test was applied to determine the significance of the data. If a non-normal distributed dataset was identified, a Kruskal-Wallis one-way analysis of variance followed by Dunn's multiple comparison test, was executed. Each experiment was repeated three independent times ($n = 3$) and all data are presented as the mean and standard error of the mean (SEM). The significance level of $\alpha = 0.05$ was applied for all statistical tests.

3. Results and discussion

3.1. Morphological characteristics of distinct embryonic stages in *E. andrei*

Based on major morphological characteristics, the development of *E. andrei* earthworm embryos can be divided into 4 major subcategories (Boros et al., 2008). E1 developmental stage corresponds to the gastrula stage, when the blastopore and the primordium of the CNS can clearly be seen under a stereomicroscope and indicate the primordium of metanephridia, while the segmentation of the body surface is absent (please see the Supplementary Material, S1A, B). During stage E2, mesodermal structures undergo pronounced differentiation, including the formation of segment boundaries (dissepiments), which extend in both anteroposterior and ventrodorsal directions, outlining the emerging body segments. It is stated that the mesodermal cell layer plays an utmost importance in shaping the earthworm body (Hunnekuhl et al., 2009). The appearance of the posteriormost segments and formation of the anal opening are morphological hallmarks of this stage. The ventral blood vessel can be followed from the 4th to the tail segment, while the dorsal one is not visible yet. From this stage, sucking and digestion of the cocoon albumen, as well as absorption of building blocks of organic compounds play an important role in the metabolic pathway and are necessary for the development of distinct tissues (Fig. S1C and D). Stage E3 embryos have an elongated, worm-like body form; however, the dorsal parts of several segments remain unclosed, creating a distinctive bulge in the middle to tail region. Probably the digestion of the sucked albumen is related to the differentiation of the alimentary canal. At this stage, both the prominent ventral and dorsal blood vessels occur within each segment; however, the dorsal vessel remains absent at the bulging region (Fig. S1E and F). By stage E4, embryos exhibit a fully elongated worm-like body form with perfectly developed segments, although the body diameter varies among specimens due to the differing amounts of albumen within the alimentary canal. In this developmental stage, not only the ventral and dorsal blood vessels but also the segmental ones are clearly distinguishable throughout the body (Fig. S1G and H).

3.2. Appearance of coelomocytes in the histological sections of different embryonic stages

The exact tissue origin of annelid coelomocytes is still debated, but a distinct hematopoietic organ, so-called “lymph gland”, has been described in several polychaetes and certain oligochaetes (Šima, 1994; Hartenstein, 2006). On the other hand, adult coelomocytes are derived from the peritoneal cells of the coelomic cavity in lumbricid earthworms (Liebmann, 1942; Jamieson, 1981; Šima, 1994). This information was supported by recent histological findings in microbe-stimulated *E. andrei* earthworms (Dvořák et al., 2016).

Maturation of coelomocytes during earthworm embryogenesis has been scarcely investigated (Santocki et al., 2014, 2016). Indeed, their sequential embryonic appearance has not yet been reported in *E. andrei* earthworms compared to the adult coelomocyte populations (Santocki et al., 2014). Our observations revealed that mesodermal cell differentiation was already evident at the E2 developmental stage, characterized by the formation of the body wall epithelium and muscle layers - key morphological indicators of embryogenesis. First, coelomocytes appeared in the anteriormost segments, which coincided with the formation of the coelomic epithelium (please see the Supplementary Material, Fig. S2A). In some sections, putative amoebocytes formed distinct rows in the coelom (Fig. S2B), whereas eleocytes or eleocyte-like cells did not occur in the coelom yet.

The E3 developmental stage had distinct body regions containing various types of coelomocytes. In completely developed segments, the differentiation of the gut epithelium and surrounding chloragocyte layer can be seen, and a high number of putative eleocytes detached into the coelom can be observed (Fig. S2C). Histological characteristics of the incomplete segments were similar to the E2 developmental stage, but they contained many more amoebocytes, forming smaller and larger cellular aggregates. Mitotic cells frequently occurred in this region as well (Fig. S2D).

In E4 developmental stage, all tissue layers displayed more advanced differentiation, accompanied by an intense expansion of chloragogenous tissue. Among chloragocytes and free-floating coelomocytes (resembling eleocytes), a high number of mitotic cells occurred (Fig. S2E). The developing chloragocytes exhibited morphological heterogeneity; some cells possessed basophilic, while others had eosinophilic cytoplasm (Fig. S2F).

3.3. Evaluation of coelomocyte subsets in E3 and E4 developmental stages

Both DIC and conventional light microscopy revealed the presence of two distinct types of coelomocytes, amoebocytes, and eleocytes in both E3 and E4 developmental stages. The size of amoebocytes varied on a large scale and most of them had granule-free cytoplasm. Some of them had cytoplasmic granules, which if present, resembled the small eleocyte granules in appearance. Eleocytes were classified into two distinct groups. The first group contained large (2-3 μm in diameter) birefringent granules, while the cytoplasm of the second one was filled with small birefringent granules of 0.5-1 μm in diameter (Fig. 1A–D). The ratio of distinct types of coelomocytes changed characteristically during embryonic development with a marked decrease of amoebocytes and a corresponding increase of the eleocytes observed in the E4 stage (Fig. 1E).

Flow cytometry analysis of adult *E. andrei* coelomocytes revealed several distinct subpopulations, which is consistent with our microscopic observations. In our earlier studies, we have identified three subpopulations denoted as R1, R2, and R3 (Engelmann et al., 2002, 2004). These populations can be classified as amoebocytes (R1 and R2) and eleocytes (R3) (Engelmann et al., 2004). Supporting our observations, Vernile et al. (2007) also measured and analyzed three coelomocyte subpopulations in adult *E. andrei* by flow cytometry. On the other hand, the flow cytometry analysis of the embryonic coelomocyte pool has been largely lacking. Following our microscopic evaluations of coelomocyte subsets from E3 and E4 embryos, we further analyzed the isolated coelomocytes from these developmental stages by flow cytometry (Fig. 1F–I). According to their light scatter-based characteristics (forward (FSC) and side scatter (SSC), respectively), the E3 embryos predominantly contained amoebocytes, whereas eleocytes were scarcely detectable (Fig. 1F). In contrast, both amoebocyte and eleocyte populations were clearly distinguishable in the E4 stage (Fig. 1G). Statistical analysis has reflected that the proportions of both amoebocyte and eleocyte subsets are gradually increased from E3 to E4 stage embryos (Fig. 1H). The statistical discrepancies in the microscopic and flow-cytometry-based evaluation of coelomocytes could be attributed to the higher sensitivity and quantitative accuracy of flow cytometry measurements compared to conventional microscopy and cell counting.

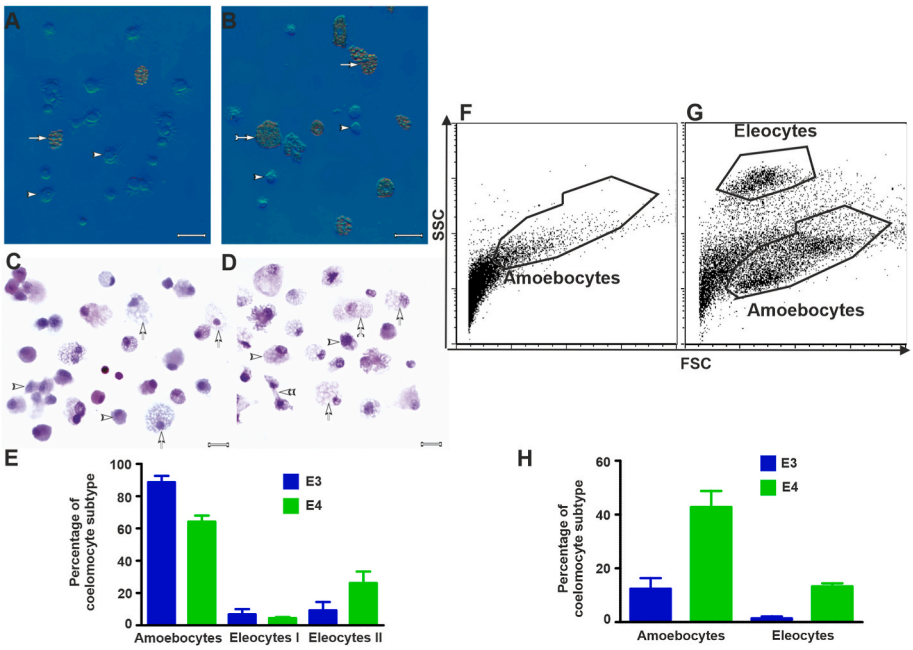

Fig. 1. Evaluation of coelomocyte parameters by DIC illumination (A, B) and conventional light microscopy (C, D). Note that in the E3 developmental stage (A, C), most of the coelomocytes are granule-free amoebocytes (arrowheads) with variable size, and only a few eleocytes (arrows) can be seen in the preparations. In the E4 developmental stage, the number of eleocytes somewhat increased, and their small granule-rich type (forked arrows) is more common than in the E3 stage. Dividing coelomocytes (double arrowheads) are also occurring in smears. Scale bars: 10 μm. Coelomocyte count (E) proves that the ratio of eleocytes increases and the ratio of amoebocytes decreases during embryonic development. Flow cytometry-based evaluation of embryonic coelomocyte subsets (F-H). Representative dot plots present the amoebocyte populations in both E3 (F) and E4 (G) stages, while the eleocyte subset occurs mostly in E4 stage (G). Bar graph (H) demonstrates the numerical representation of coelomocyte subsets in the different embryonic stages (n = 3, mean +SEM).

3.4. Evolution of PRR and AMP gene expression during E. andrei embryogenesis

Invertebrate innate immune response is initiated by ligand engagements mediated by pattern recognition receptors (PRRs), which subsequently triggers intracellular signal transduction pathways, similar to those observed in vertebrates' innate immunity. Over the past decades, several PRR molecules have been identified and characterized from the earthworm *E. andrei* (Bilej et al., 2018). Among those, coelomic cytolytic factor (CCF) represents a unique PRR, discerned in several earthworm species (Procházková et al., 2020), while others, such as toll-like receptors (TLRs), lipopolysaccharide-binding protein/bactericidal/permeability-increasing protein (LBP/BPI), scavenger receptors (SRs), and peptidoglycan-recognition proteins (PGRPs) are well conserved across both invertebrate and vertebrate taxa (Silva and Gomes, 2024). Following microbial or damaged-self ligand binding, PRRs trigger the release of various soluble mediators, including growth factors, cytokines and antimicrobial peptides (Canesi et al., 2022).

However, the embryonic expression pattern of these PRRs and soluble mediators remains largely obscured during earthworm development. In this regard, we have quantified the total embryonic transcript levels of several immune receptors and effector molecules throughout *E. andrei* ontogenesis. *CCF* expression revealed low/undetectable levels (Fig. 2A) during the E1-E3 stages but showed a significant upregulation at E4 stage. In contrast, *LBP/BPI* expression displayed a gradual and significant decline from E1 to E4 stages (Fig. 2B). The mRNA expression of *TLR* and the signal adaptor *MyD88* (of the TLR signaling pathway) was evident in all four embryonic stages (Fig. 2C and D). Just recently, a novel member of the multiple cysteine cluster (mcc) TLR has been described in *E. andrei* earthworms (Procházková et al., 2019). The first characterized earthworm TLR, *Ea*TLR, is ubiquitously expressed in several adult earthworm tissues, while mccTLR expression was mostly restricted to seminal vesicles and receptacles (Bilej et al., 2018). The mccTLR was reported to be expressed during early stages of development, while *Ea*TLR was mainly present in adult stages (Procházková et al., 2019). In contrast, we have detected the presence of *EaTLR* in all four embryonic stages, which could be explained by the ubiquitous expression of EaTLR. On the other hand, several TLR variants are present in earthworm genome (Fjøsne et al., 2015) that are partially unknown and might also influence our findings. *Scavenger receptor* (SR) mRNA expression has followed a similar trend compared to *CCF,* showing an undetectable or very low amount in E1-E3 embryos, followed by a significant upregulation in the E4 stage (Fig. 2E).

Subsequently, we quantified the mRNA expression levels of the antimicrobial proteins *lysenin* and *lysozyme*. *Lysenin* transcripts were undetectable during E1 and E2 stages, but they increased markedly by E3 and reached significant elevation in E4 stage (Fig. 2F). In contrast, *lysozyme* mRNA level demonstrated a gradual increase throughout embryogenesis from E1 to E4 (Fig. 2G). In addition, lysozyme protein expression has also been detected in the cocoons of *Dendrobaena veneta* (Fiołka et al., 2012). Earlier, we identified and characterized the homologues of *lumbricin* and *lumbricin-related protein (LuRP)* mRNA in *E. andrei* earthworm (Bodó et al., 2019). Both *lumbricin* and *LuRP* mRNA transcripts showed a gradual increase from E1 to E4 stages during *Eisenia* ontogenesis; however, LuRP expression was consistently higher compared to *lumbricin.* In contrast, Lumbricin I, isolated from *Lumbricus rubellus* has exhibited detectable RNA expression only in adult earthworms (Cho et al., 1998).

Although the different PRR molecules are subject to variable expression patterns during embryogenesis, we can conclude that AMP expression generally evidenced a gradual increase from E1 to E4 stages.

4. Conclusions

Earthworm embryos revealed a sequential appearance of amoebocytes *vs.* eleocytes during embryogenesis in *Eisenia andrei.* Amoebocytes, which mediate distinct cellular immune functions emerged first, while eleocytes, which are primarily involved in humoral immunity, emerged

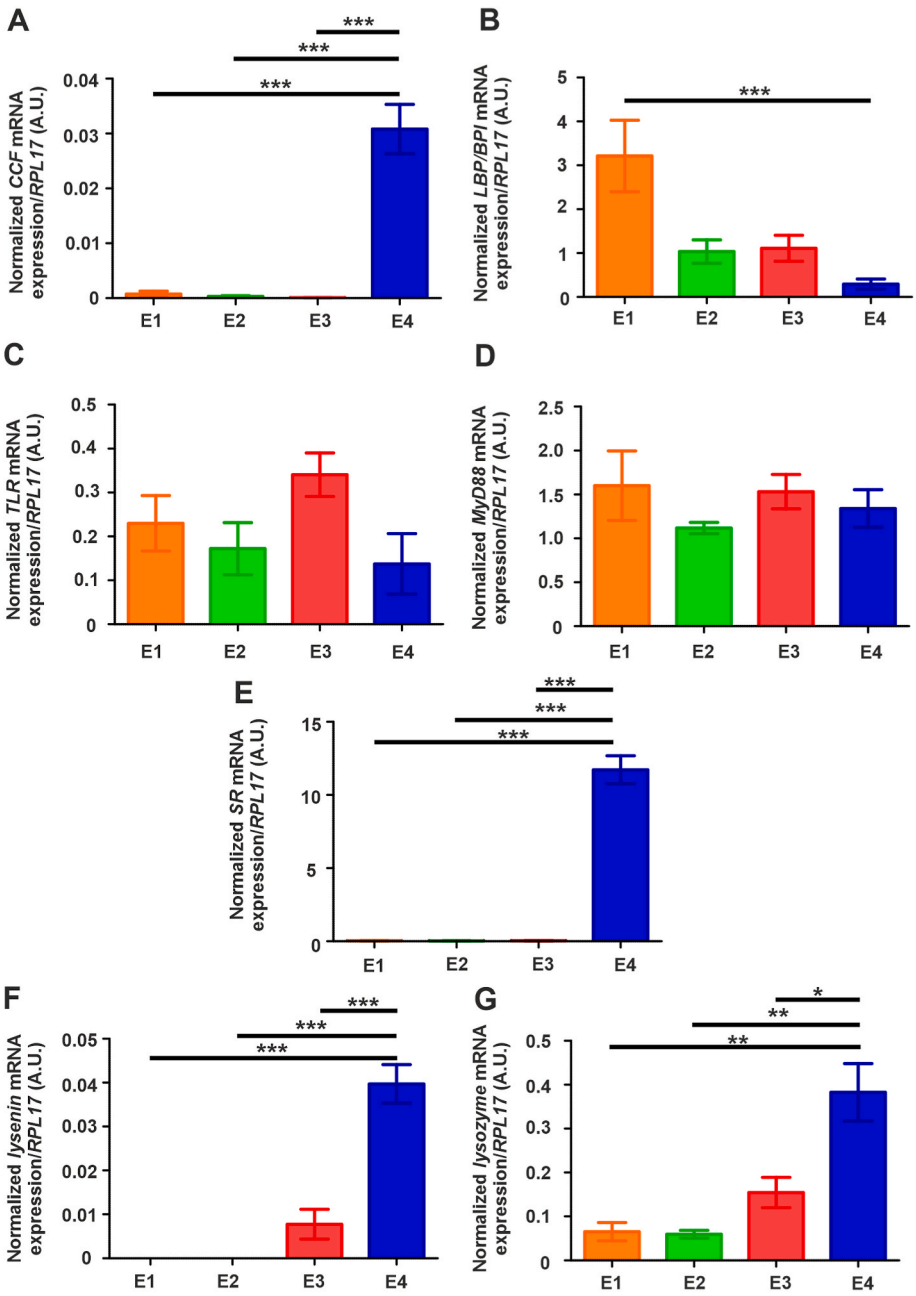

Fig. 2. Differential expression levels of immune response-related genes (**A**: *CCF;* **B**: *LBP/BPI*, **C**: *TLR*, **D**: *MyD88,* **E**: *SR*, **F**: *lysenin*, **G**: *lysozyme*) during the developmental stages of *E. andrei* earthworm embryogenesis. Quantitative measurements were normalized to *E. andrei RPL17* mRNA levels. Relative expression values are given as mean ± SEM. Three independent experiments were performed in duplicates. Asterisks represent significant p values (*< 0.05, **< 0.01, *** < 0.001, Kruskal-Wallis).

later. This temporal dichotomy was also reflected in the gene expression patterns: PRRs (e.g. TLR, LBP/BPI), which are responsible for microbial recognition, were generally expressed earlier in the ontogenesis, whereas humoral factors (e.g. lysenin), responsible for antimicrobial activity, were produced during the advanced embryonic developmental stages.

CRediT authorship contribution statement

Kornélia Bodó: Writing – original draft, Methodology, Investigation, Formal analysis, Conceptualization. **Bohdana Kokhanyuk:** Writing – review & editing, Methodology, Formal analysis. **Dániel Dunai:** Resources. **Chayeen Brotzki da Costa:** Writing – review & editing, Methodology, Formal analysis. **Éva Rumpler:** Writing – review & editing, Formal analysis. **Zoltán Kopasz:** Resources. **Edit Pollák:** Supervision, Resources. **Péter Németh:** Writing – review & editing, Resources. **László Molnár:** Writing – review & editing, Supervision, Resources, Methodology, Investigation, Formal analysis, Data curation, Conceptualization. **Péter Engelmann:** Writing – original draft, Visualization, Supervision, Resources, Methodology, Investigation, Funding acquisition, Formal analysis, Conceptualization.

Acknowledgements

This research was funded by the University of Pécs (020_2024_PTE_RK/7, 020_2024_PTE_RK/36, 003_2025_PTE_RK/9, 003_2025_PTE_RK/10), EKÖP-24-4-II-PTE-130, GINOP-232-15-2016-00050, EFOP-361-16-2016-00004. Project No. TKP2021-EGA-10 has

been implemented with the support provided by the Ministry of Culture and Innovation of Hungary from the National Research, Development and Innovation Fund, financed under the TKP2021 funding scheme. The work was supported by the ÚNKP-19-3-I New National Excellence Program of the Ministry for Innovation and Technology, K.B.; and National Brain Project (NAP2022-I-10/2022, HUN-REN BLRI), Laboratory of Water Science and Water Security (RRF 2.3.1-21-2022-00008, HUN-REN, BLRI).

Appendix A. Supplementary data

Supplementary data to this article can be found online at https://doi.org/10.1016/j.dci.2026.105578.

Data availability

Data will be made available on request.

References

Bergter, A., Beck, L.A., Paululat, A., 2004. Embryonic development of the oligochaete *Enchytraeus coronatus*: an SEM and histological study of embryogenesis from one-cell stage to hatching. J. Morphol. 261, 26–42. https://doi.org/10.1002/jmor.10189.

Bilej, M., Procházková, P., Roubalová, R., Škanta, F., Dvořák, J., 2018. Recognition of nonself in earthworms. In: Cooper, E.L. (Ed.), Advances in Comparative Immunology. Springer Verlag, pp. 161–173. https://doi.org/10.1007/978-3-319-76768-0_7.

Bodó, K., Boros, Á., Rumpler, É., Molnár, L., Böröcz, K., Németh, P., Engelmann, P., 2019. Identification of novel lumbricin homologues in *Eisenia andrei* earthworms. Dev. Comp. Immunol. 90, 41–46. https://doi.org/10.1016/j.dci.2018.09.001.

Boros, Á., Reglödi, D., Herbert, Z., Kiszler, G., Németh, J., Lubics, A., Kiss, P., Tamás, A., Shioda, S., Matsuda, K., Pollák, E., Molnár, L., 2008. Changes in the expression of PACAP-like compounds during the embryonic development of the earthworm *Eisenia fetida*. J. Mol. Neurosci. 36, 157–165. https://doi.org/10.1007/s12031-008-9102-6.

Canesi, L., Auguste, M., Balbi, T., Prochazkova, P., 2022. Soluble mediators of innate immunity in annelids and bivalve mollusks: a mini-review. Front. Immunol. 13, 1051155. https://doi.org/10.3389/fimmu.2022.1051155.

Cooper, E.L., Stein, E.A., 1981. Oligochaetes. In: Ratcliffe, N.A., Rowley, A.F. (Eds.), Invertebrate Blood Cells. Academic Press, pp. 75–140.

Cho, J.H., Park, C.B., Yoon, Y.G., Kim, S.C., 1998. Lumbricin I, a novel proline-rich antimicrobial peptide from the earthworm: purification, cDNA cloning and molecular characterization. Biochim. Biophys. Acta 1408, 67–76. https://doi.org/10.1016/S0925-4439(98)00058-1.

Dvořák, J., Roubalová, R., Procházková, P., Rossmann, P., Skanta, F., Bilej, M., 2016. Sensing microorganisms in the gut triggers the immune response in *Eisenia andrei* earthworms. Dev. Comp. Immunol. 57, 67–74. https://doi.org/10.1016/j.dci.2015.12.001.

Endo, M., Sakai, C., Shimizu, T., 2016. Embryonic expression patterns of Hox genes in the oligochaete annelid *Tubifex tubifex*. Gene Expr. Patterns 22, 1–14. https://doi.org/10.1016/j.gep.2016.09.002.

Engelmann, P., Pál, J., Berki, T., Cooper, E.L., Németh, P., 2002. Earthworm leukocytes react with different mammalian antigen-specific monoclonal antibodies. Zool. 105, 257–265. https://doi.org/10.1078/0944-2006-00068.

Engelmann, P., Molnár, L., Pálinkás, L., Cooper, E.L., Németh, P., 2004. Earthworm leukocyte populations specifically harbor lysosomal enzymes that may respond to bacterial challenge. Cell Tissue Res. 316, 391–401. https://doi.org/10.1007/s00441-004-0874-x.

Engelmann, P., Pálinkás, L., Cooper, E.L., Németh, P., 2005. Monoclonal antibodies identify four distinct annelid leukocyte markers. Dev. Comp. Immunol. 29, 599–614. https://doi.org/10.1016/j.dci.2004.10.008.

Engelmann, P., Hayashi, Y., Bodó, K., Ernszt, D., Somogyi, I., Steib, A., Orbán, J., Pollák, E., Nyitrai, M., Németh, P., Molnár, L., 2016. Phenotypical and functional characterization of earthworm coelomocyte subsets: linking light-scatter based cell typing and imaging the sorted populations. Dev. Comp. Immunol. 65, 41–52. https://doi.org/10.1016/j.dci.2016.06.017.

Fiołka, M.J., Zagaja, M.P., Hułas-Stasiak, M., Wielbo, J., 2012. Activity and immunodetection of lysozyme in earthworm *Dendrobaena veneta*. (Annelida). J. Invertebr. Pathol. 109, 83–90. https://doi.org/10.1016/j.jip.2011.10.002.

Fjøsne, T.F., Stenseth, E.B., Myromslien, F., Rudi, K., 2015. Gene expression of TLR homologues identified by genome-wide screening of the earthworm *Dendrobaena veneta*. Innate Immun. 21, 161–166. https://doi.org/10.1177/1753425914523O.

Hartenstein, V., 2006. Blood cells and blood cell development in the animal kingdom. Annu. Rev. Cell Dev. Biol. 22, 677–712. https://doi.org/10.1146/annurev.cellbio.22.010605.093317.

Homa, J., 2018. Earthworm coelomocyte extracellular traps: structural and functional similarities with neutrophil NETs. Cell Tissue Res. 371, 407–414. https://doi.org/10.1007/s00441-018-2787-0.

Hunnekuhl, V.S., Bergter, A., Purschke, G., Paululat, A., 2009. Development and embryonic pattern of body wall musculature in the crassiclitellate *Eisenia andrei* (Annelida, Clittelata). J. Morphol. 270, 1122–1136. https://doi.org/10.1002/jmor.10749.

Jamieson, B.G.M., 1981. Coelomocytes. In: Jamieson, B.G.M. (Ed.), The Ultrastructure of the Oligochaete. Academic Press, New York, pp. 62–95.

Koza, A., Wilhelm, M., Hiripi, L., Elekes, K., Csoknya, M., 2006. Embryogenesis of the serotonergic system in the earthworm *Eisenia fetida* (Annelida, Oligochaeta): immunhistochemical and biochemical studies. J. Comp. Neurol. 497, 451–467. https://doi.org/10.1002/cne.21008.

Liebmann, E., 1942. The coelomocytes of Lumbricidae. J. Morphol. 71, 221–249.

Matsuo, K., Yoshida, H., Shimizu, T., 2005. Differential expression of *caudal* and *dorsal* genes in the teloblast lineages of the oligochaete annelid *Tubifex tubifex*. Dev. Gene. Evol. 215, 238–247. https://doi.org/10.1007/s00427-005-0473-1, 2005.

Molnár, L., Engelmann, P., Somogyi, I., Mácsik, L.L., Pollák, E., 2012. Cold-stress induced formation of calcium and phosphorous rich chloragocyte granules (chloragosomes) in the earthworm *Eisenia fetida*. Comp. Biochem. Physiol. 163A, 199–209. https://doi.org/10.1016/j.cbpa.2012.06.005.

Opper, B., Bognár, A., Heidt, D., Németh, P., Engelmann, P., 2013. Revising lysenin expression of earthworm coelomocytes. Dev. Comp. Immunol. 39, 214–218. https://doi.org/10.1016/j.dci.2012.11.006.

Procházková, P., Roubalová, R., Škanta, F., Dvořák, J., Navarro Pacheco, N.I., Kolarik, M., Bilej, M., 2019. Developmental and immune role of a novel multiple cysteine cluster TLR from *Eisenia andrei* earthworms. Front. Immunol. 10, 1277. https://doi.org/10.3389/fimmu.2019.01277.

Procházková, P., Roubalóvá, R., Dvořák, J., Navarro Pacheco, N.I., Bilej, M., 2020. Pattern recognition receptors in annelids. Dev. Comp. Immunol. 102, 103493. https://doi.org/10.1016/j.dci.2019.103493.

Santocki, M., Falniowski, A., Plytycz, B., 2016. Restoration of experimentally depleted coelomocytes in juvenile and adult composting earthworms *Eisenia andrei, E. fetida, Dendrobaena veneta*. Appl. Soil Ecol. 104, 163–173. https://doi.org/10.1016/j.apsoil.2015.08.022.

Santocki, M., Klimek, M., Kruk, J., Plytycz, B., 2014. Preliminary report on coelomocyte system during ontogeny of the earthworm *Dendrobaena veneta*. Acta Biolog. Cracow 55–56, 65–71.

Shimizu, T., Nakamoto, A., 2001. Segmentation in annelids: cellular and molecular basics for metameric body plan. Zool. Sci. 18, 285–298. https://doi.org/10.2108/zsj.18.285.

Shankland, M., Seaver, E.C., 2000. Evolution of the bilaterian body plan: what have we learned from annelids? Proc. Natl. Acad. Sci. USA. 97, 4434–4437. https://doi.org/10.1073/pnas.97.9.4434.

Silva, R.C.M.C., Gomes, F.M., 2024. Evolution of the major components of innate immunity in animals. J. Mol. Evol. 92, 3–20. https://doi.org/10.1007/s00239-024-10155-2, 2024.

Šima, P., 1994. Annelid coelomocytes and hemocytes: roles in cellular immune reactions. In: Vetvicka, V., Sima, P., Cooper, E.L., Bilej, M., Roch, P. (Eds.), Immunology of Annelids. CRC Press, Boca Raton, pp. 115–164.

Vernile, P., Fornelli, F., Bari, G., Spagnuolo, M., Minervini, F., de Lillo, E., Ruggiero, P., 2007. Bioavailability and toxicity of pentachlorophenol in contaminated soil evaluated on coelomocytes of *Eisenia andrei* (Annelida, Lumbricidae). Toxicol. Vitro 21, 302–307. https://doi.org/10.1016/j.tiv.2006.09.026.

Vetvicka, V., 1994. Physiology of annelids. In: Vetvicka, V., Sima, P., Cooper, E.L., Bilej, M., Roch, P. (Eds.), Immunology of Annelids. CRC Press, Boca Raton, pp. 41–113.